Uniplanar deformation of isotactic polypropylene: 1. Draw characteristics

Satoshi Osawa* and Roger S. Porter†
Polymer Science and Engineering Department, University of Massachusetts, Amherst, MA 01003, USA
(Received 9 November 1992; revised 24 February 1993)

Isotactic polypropylene (iPP) ($M_w = 2.9 \times 10^5$) has been deformed in uniaxial compression by forging at several constant temperatures from 20 to 140°C. A relation between draw efficiency and the formation of the smectic phase during deformation has been examined over a wide range of compression draw ratios (~50). At a forging temperature below the smectic-phase stability limit temperature (T_s), the efficiency of draw, parallel to the uniplanar direction, was high (~97%) and independent of the compression ratio, pressure and draw temperature (T_d). The relation between the compression yield energy (E_y) and T_d has also been examined. E_y, the area under the compressive stress–strain curve up to the yield point, as a function of T_d was found to consist of two linear components of different slope. These two linear relations arose from the glassy and crystalline phases. The intercept temperature (T_i) at zero yield energy for the glassy phase has been evaluated to understand compression drawability. Above T_i, the achievable compression ratio (CR) increased steadily with T_d. At a given T_d, the CR increased with increasing applied pressure, and this tendency was more prominent above T_i. The T_i moved higher as the compression rate was increased.

(Keywords: planar deformation; draw efficiency; isotactic polypropylene)

INTRODUCTION

A uniaxial compression (forging) experiment has been used in this laboratory to study the uniplanar deformation of isotactic polypropylene (iPP) in the solid state[1,2]. A previous study[3] reported that compression deformation induced a smectic phase. The upper temperature limit for stability of the smectic phase (T_s) was found to increase by increasing the deformation rate and pressure. Further, the X-ray pole density distribution experiment showed more crystal orientation in the sample prepared below T_s than above T_s. However, a quantitative estimation of draw efficiency and its dependence on draw ratio has not yet been carried out. Planar deformation is induced under high pressure (~1 GPa), i.e. $\sim 10^4$ times atmospheric. This pressure during deformation also affects chain mobility and the glass transition temperature (T_g). Thus, for understanding deformation, it is necessary to estimate the T_g under compression as well as the T_s.

In this study, a quantitative estimation of the overall drawing efficiency, including the amorphous phase, has been carried out based on shrinkage parallel and perpendicular to the compression direction. Further, the rheology of the process has been examined from the compression yield energy as a function of the compression rate and the draw temperature. Based on the results, the compression draw is characterized.

* Present address: Department of Materials Science and Technology, Science University of Tokyo, Yamaguchi College, Daigakudori, Onodashi, Yamaguchi 756, Japan
† To whom correspondence should be addressed

0032-3861/94/030540–05

EXPERIMENTAL

The isotactic polypropylene (iPP) used in this study (supplied by Philips Co.) had a melt index of 4.0 corresponding to a molecular weight, M_w, of 2.9×10^5. The peak melting point was ~163°C. The original pellets were moulded into a sheet of thickness 5.6 mm in a vacuum press at 220°C. The mould was quenched by ice-water. From wide-angle X-ray analysis, the crystals were found to be of an α-form with no measurable smectic-phase content. The moulded sheets were uniaxially compressed under isothermal conditions at temperatures from 20 to 140°C, using a dynamic test system composed of an INSTRON Model 1333 which allows on-line measurement of load and displacement during the deformation process. For lubricated deformation, a drop of silicon oil was placed on each side of the sample surface before compression. The forging experiment consists of squeezing the polymer out of the compression zone. The compression area (~2.5 cm diameter cylinder) remains unchanged during forging. A detailed description has been given elsewhere[1].

Thermal analyses were performed on a Perkin–Elmer DSC7 calorimeter. All scans were recorded at a heating rate of 20°C min^{-1}. Shrinkage experiments were performed at several constant temperatures. Samples are immersed in a silicone oil bath for sufficient time (depending on the test temperature) to reach shrinkage equilibrium. For measurement of full recovery, thermal shrinkage was performed at high temperature (220°C) to achieve a rapid shrink of the sample. The percentage

elastic recoveries parallel, $R(3)$, and perpendicular $R(2)$, to the compression direction, and the area recovery, $R(1)$, were evaluated. $R(1)$, $R(2)$ and $R(3)$ were defined (in %) as follows:

$$R(1)=\frac{S_c-S_s}{S_c-S_o}\times 100=\frac{S_c-S_s}{S_c(1-CR^{-1})}\times 100 \quad (1)$$

$$R(2)=\frac{L_c-L_s}{L_c-L_o}\times 100=\frac{L_c-L_s}{L_c(1-CR^{-1/2})}\times 100 \quad (2)$$

$$R(3)=\frac{d_s-d_c}{d_o-d_c}\times 100=\frac{d_s-d_c}{d_c(CR-1)}\times 100 \quad (3)$$

The sample dimensions before compression, and before and after shrink are defined in *Figure 1*, where $CR=d_o/d_c$ is the compression ratio, and $DR=L_c/L_o$ is the draw ratio parallel to the uniplanar direction. Since compression experiments (forging) consist of squeezing the polymer out of the compression zone, S_o and L_o cannot be measured directly.

In solid-state deformation of iPP, the density of the samples before and after compression is similar, i.e. volume conservation can be assumed for draw calculations. Thus, $CR=DR^2=S_c/S_o$ is assumed. *Figure 2* shows the relation between DR and CR. The DR was measured by the distance between marks scratched on the sample surface before and after deformation. A straight line, $DR^2=CR$ (or $DR=CR^{1/2}$), was realized within experimental error, independent of deformation temperature and CR. The solid line does not reveal 100% efficient draw of molecules, but a uniform deformation on a macroscopic scale.

The extent of deformation can best be expressed by a molecular draw ratio MDR[4,5]. In uniaxial compression, $DR=CR^{1/2}$ gives the MDR parallel to the draw direction as follows:

$$MDR=\frac{L_c-L_s+L_o}{L_o}=\frac{L_c-L_s}{L_c}CR^{1/2}+1 \quad (4)$$

Then draw efficiency in the uniplanar direction is given by $(MDR)^2/CR$.

RESULTS AND DISCUSSION

On uniaxial compression of iPP, the smectic phase is induced at a draw temperature below ~120°C (T_s) at a constant compression speed of 0.254 cm min^{-1} (ref. 3). The crystal orientation of the sample obtained below T_s is higher than that above T_s at the same compression ratio[3]. In order to investigate the effects of draw temperature, T_d, (related to T_s) and CR on the overall deformation efficiency, including the amorphous phase, two shrinkage experiments have been carried out. One is to determine the MDR defined by equation (4). The other involves recovery tests defined by equations (1)–(3).

Figure 3 shows $(MDR)^2$ parallel to the uniplanar draw direction as a function of CR for T_d of 50, 100 ($<T_s$) and 140°C ($>T_s$). The compression speed is 0.254 cm min^{-1}. Here, the draw efficiency is $(MDR)^2/CR$. This estimation is based on the sample shrink perpendicular to the compression direction. The solid line represents an affine deformation, the situation where $(MDR)^2=CR$, i.e. for 100% efficient draw. For T_d of 50 and 100°C ($<T_s$), the deformation is found to be highly efficient, ~97%. Further, the efficiency is independent of CR. This suggests that affine deformation proceeds in both the amorphous and crystalline phases. At 140°C ($>T_s$), the relation between $(MDR)^2$ and CR is also linear; however, the

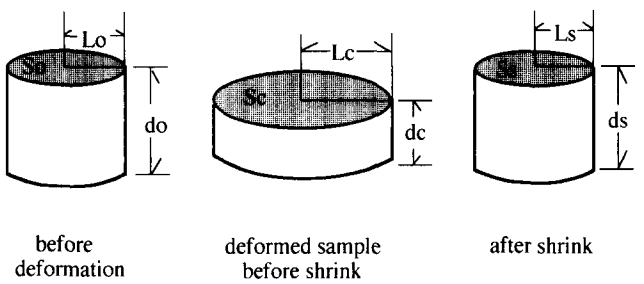

Figure 1 Sample dimensions before and after compression, and after shrink

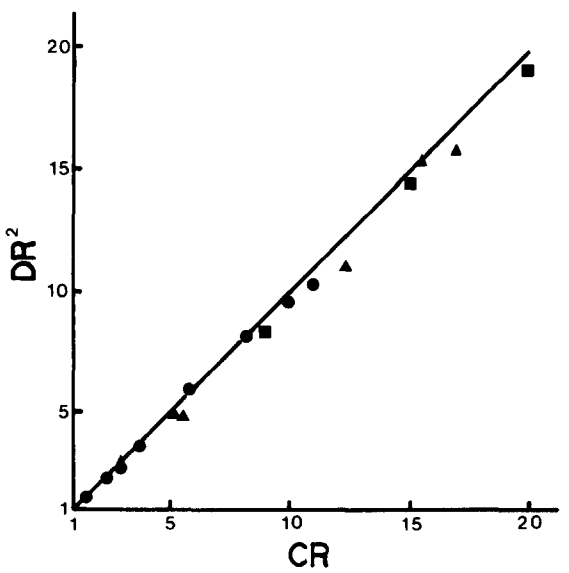

Figure 2 DR^2 *versus* CR at compression temperatures of 50 (●), 100 (▲) and 140°C (■). Compression speed was 0.254 cm min^{-1}

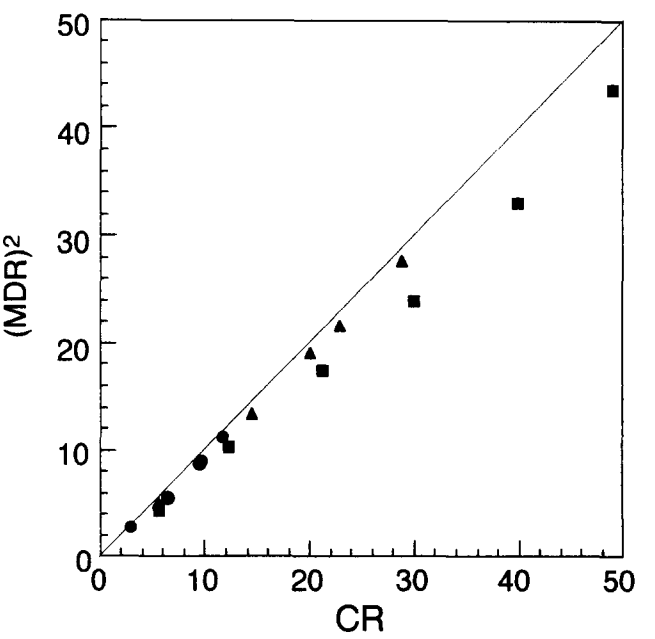

Figure 3 $(MDR)^2$ parallel to the uniplanar direction *versus* CR for samples prepared at 50 (●), 100 (▲) and 140°C (■)

average efficiency (82%) is lower than at 50 and 100°C ($< T_s$).

The thermal behaviour of the compressed sample has also been examined from the elastic recovery parallel, $R(3)$, and perpendicular, $R(2)$, to the compression direction, and from the area recovery, $R(1)$, as a function of temperature. To understand which definition of R is available to estimate compression efficiency, the relations between $R(1)$, $R(2)$ and $R(3)$ are considered (see Appendix):

$$R(1) = CR\frac{1-Cr^{-1}}{Cr-1}R(3) \quad (5)$$

$$R(2) = (CR+CR^{1/2})\frac{1-Cr^{-1/2}}{Cr-1}R(3) \quad (6)$$

where $Cr = d_s/d_c = S_c/S_s = (L_c/L_s)^2$.

Figures 4a and *4b* show $R(1)$ and $R(2)$ as a function of $R(3)$, respectively. The solid lines are calculated from equations (5) and (6) at several values of CR. The plotted data were measured on a sample with a compression ratio of 9.6, and agree with calculations from equations (5) and (6). These results show that at the initial stage of sample shrinkage, $R(1)$ and $R(2)$ change more than $R(3)$.

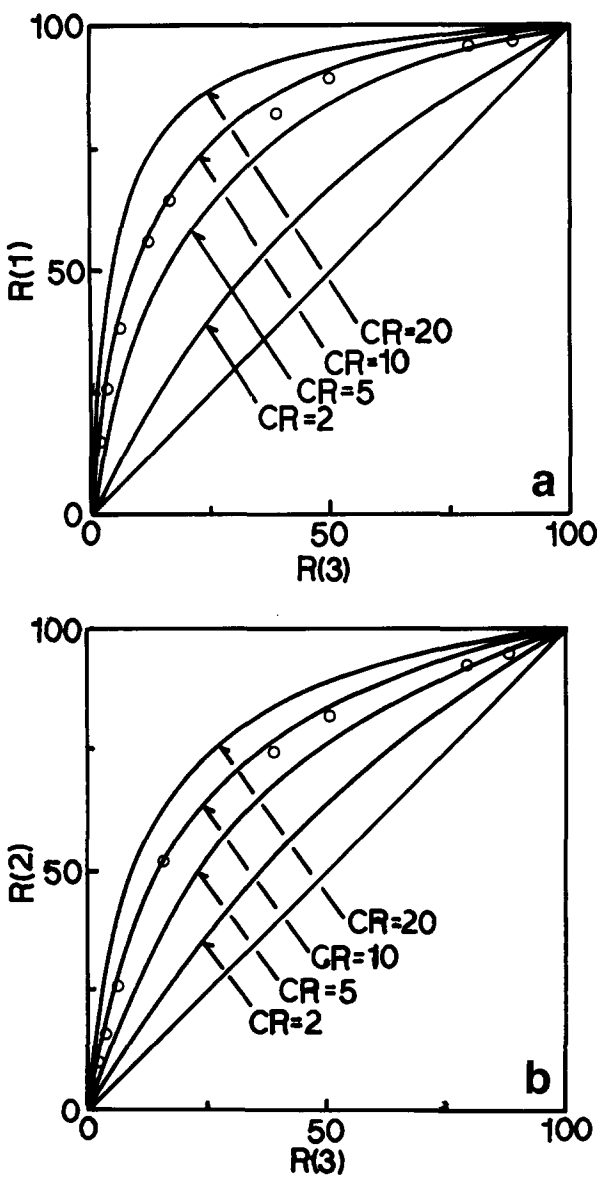

Figure 4 Relation between (a) $R(1)$ and $R(3)$, and (b) $R(2)$ and $R(3)$

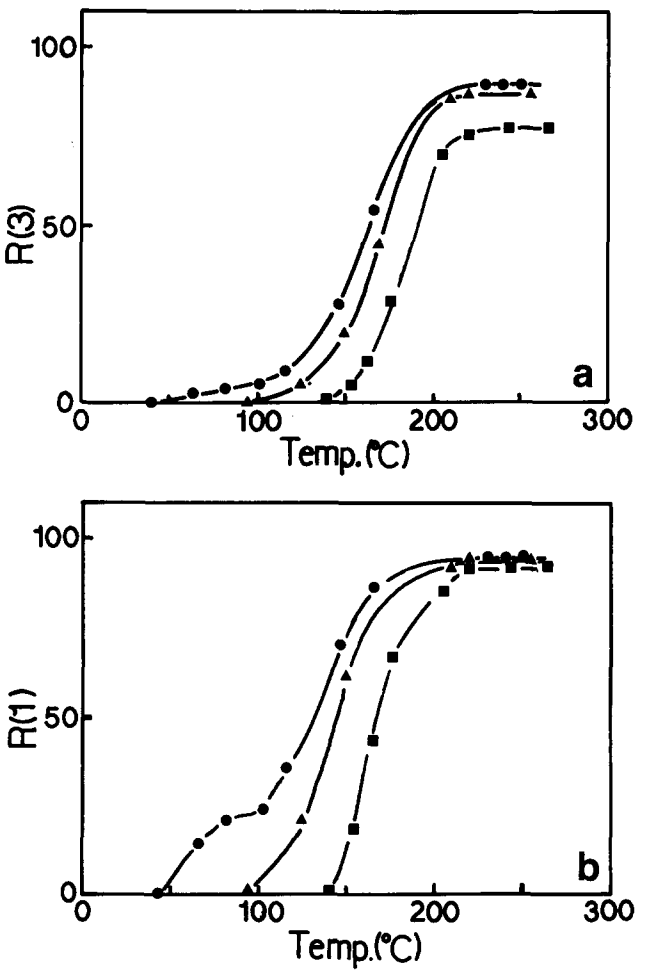

Figure 5 (a) $R(3)$ and (b) $R(1)$ *versus* temperature for samples prepared at 50 (●), 100 (▲) and 140°C (■) at CR of 6.7, 6.2, and 5.6, respectively. Compression speed was 0.254 cm min^{-1}

In contrast, at a later stage of elastic recovery, $R(1)$ and $R(2)$ change less. Therefore, $R(1)$ and $R(2)$ are sensitive for evaluation of the early stages of shrinkage, whereas the $R(3)$ shrinkage test is more sensitive for evaluation of full recovery.

To estimate draw efficiency, full recovery on melting is required. Therefore, the $R(3)$ test is chosen for the estimation of the compression efficiency. The $R(3)$ test is based on sample expansion along the compression direction on heating. *Figure 5a* shows $R(3)$ as a function of temperature for samples prepared at 50, 100 and 140°C at a CR of 6.7, 6.2 and 5.6, respectively. Here, the final recovery of $R(3)$ reveals the compression draw efficiency. It can be seen that values of $R(3)$ for $T_d = 50$ and 100°C ($< T_s$) are high ($\sim 90\%$). However, for $T_d = 140$°C ($> T_s$), the value drops to $\sim 75\%$. This is associated with the results from *MDR*. Thus, draw efficiency both parallel and perpendicular to the compression direction below T_s is higher than that above T_s at any CR in this experimental region. The α-form crystal changes to the smectic phase during deformation at $T_d < T_s$, which would lead to a highly efficient draw.

Figure 5b shows $R(1)$ as a function of temperature for samples prepared under the same conditions as in *Figure 5a*. As expected, the $R(1)$ test is not suitable for estimating full recovery, but gives some information about the onset of sample shrinkage. The compressed iPP samples are found to exhibit some shrink at about draw temperature, that is at the temperature that they had been drawn and annealed in compression. The peak

melting points of the samples measured by d.s.c. were ~160–165°C and the onset temperatures were ~148–152°C. Therefore, the elastic recovery below the onset temperature is mainly due to the recovery of the amorphous region. For maximum thermal stability, it is necessary to conduct the compression draw at a temperature as high as possible yet below the melting point.

The crystallinity of the original sample was about half of the α-form plus half of the amorphous phase. As the T_d is decreased, the amorphous chain mobility is reduced, leading to less drawability. Below and above T_g, the ductility must be quite different. Macosko and Brand[6] reported a linear relation between the energy to yield and the test temperature on tensile testing of several amorphous polymers. They showed that the tensile yield energy goes to zero at T_g, according to the following relation:

$$E_y = \int_0^{\varepsilon_y} \sigma \, d\varepsilon = A(T_g - T) \qquad (7)$$

where E_y is the yield energy, ε the strain, ε_y the strain at the yield point, σ the stress, and A is a constant. Equation (7) has been theoretically[7,8] and experimentally[9,10] discussed for many glassy polymers. In order to obtain information about T_g under deformation, yield energy as a function of T_d is examined for this compression system.

Figure 6 shows plots of E_y *versus* T_d at compression speeds of 0.254 and 0.0254 cm min^{-1}. The yield energy defined by equation (7) is taken as the area under the curve up to the yield point. The point where the stress–strain curve goes through a maximum was chosen as the compression yield point. For each speed, the relation between E_y and T_d consists of two linear components. Thus, equation (7) does not cover the results from below T_g up to T_m. For a semicrystalline polymer, Hartmann and Cole[10] showed that the yield energy was also a linear function of temperature above T_g:

$$E_y = B(T_m - T) \qquad (> T_g) \qquad (8)$$

where B is a constant. Since the polymer tested in this study is semicrystalline, equation (8) is applicable above T_g. Below T_g, the addition of equations (7) and (8) would be useful for understanding yield behaviour:

$$E_y = A(T_g - T) + B(T_m - T) \qquad (< T_g) \qquad (9)$$

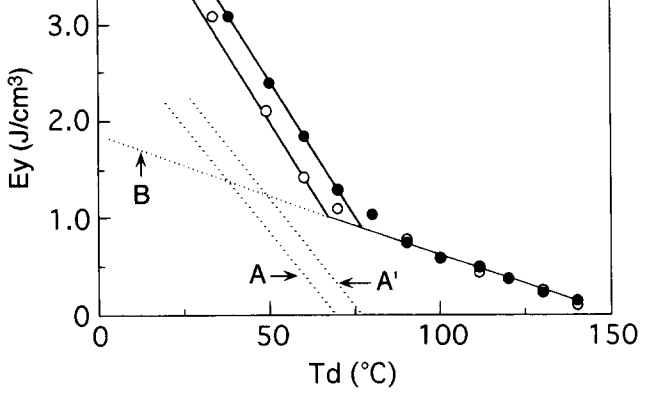

Figure 6 E_y *versus* T_d for compression speeds: (●) 0.254; (○) 0.0254 cm min^{-1}. The dotted lines A (or A') and B represent the components from the first and second terms of equation (9), respectively. A and A' are for higher and lower compression speeds, respectively

The two linear slopes for each compression speed observed in *Figure 6* are characterized by equations (8) and (9). From equation (8), the intercept temperature (for line B) at zero yield energy is 152°C, which is associated with the onset temperature of melting. In equation (9), the first and second terms are revealed by the dotted lines of A (or A') for the glassy phase and B for the crystalline phase, respectively. The intercept temperatures of lines A and A' at $E_y = 0$ are 67 and 77°C for compression speeds of 0.254 and 0.0254 cm min^{-1}, respectively. Those intercept temperatures (T_i) do not correspond to ambient T_g of iPP (~0°C)[11,12]. Beatty and Weaver[9] pointed out that the effect of strain rate on the T_i of a glassy polymer evaluated from equation (7) was small for tensile deformation, whereas for compression deformation, increasing the strain rate shifts the intercept temperature to higher values; e.g. for polystyrene there was a shift in the intercept temperature of ~100 K for a ten-fold increase in the compressive strain rate compared to a 7 K shift in the tensile strain rate. Thus, T_i in the compression process evaluated from equation (9) is much higher than the polymer ambient T_g. T_g also increases both with the compression pressure and the rate of testing. Most workers[13,14] found the pressure dependence on T_g (dT_g/dp) to be of the order of ~0.015–0.035°C kg^{-1} cm^2. In this study, the yield stress at room temperature was ~3.0×10^7 Pa for 0.254 cm min^{-1}. Taking those values, the T_g shift by the pressure is approximately 4.5–10.5°C. Therefore, the main reason that T_i is observed at a higher temperature than the ambient T_g might be due to the strain rate.

From the slope of each line in *Figure 6*, a fraction ratio (b/b') of thermal energy (b) and mechanical energy (b') to overcome the activation energy barrier for flow has been estimated for both compression and tensile deformation. The slope is expressed by $(b/b')\rho C_p^7$, where ρ is the average density and C_p is the average heat capacity per unit mass. For both compression speeds, the slope below T_i is four times higher than that above T_i, i.e. b/b' below T_i is four times higher than that above T_i. This means that above T_i stress enhances the flow in the direction of deformation more effectively than it does below T_i[9]. It is noted that T_i shifts to higher values with increasing compression speed.

The attainable CR for iPP is controlled by T_d and the pressure applied during deformation. *Figure 7* shows the CR *versus* $T_d - T_i$ at several applied deformation pressures. Above T_i ($T_d - T_i > 0$), the achievable CR increased steadily with temperature. Below T_i, the increase in CR with temperature is minor. Further, samples sometimes exploded with the pressure above 0.2 GPa. At a given T_d, the increase in CR with pressure above T_i is more than that below T_i. Thus, T_i on the compression draw is an important factor in understanding the compression drawability. The effects of T_d on drawability and draw efficiency are summarized in *Table 1*. By performing the deformation at temperatures above T_i and below T_s, extremes of uniplanar draw are achieved with high draw efficiency, as measured by elastic recovery on melting. It may also be noted that both T_i and T_s are functions of compression speed.

The structures and properties of forged iPP samples will appear in companion papers.

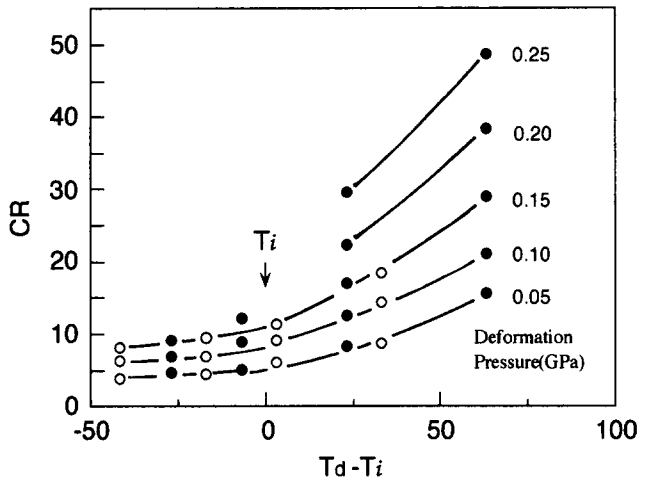

Figure 7 *CR versus* $T_d - T_i$ at the indicated applied pressures for compression speeds (●) 0.254; (○) 0.0254 cm min^{-1}

Table 1 Polypropylene compressive draw characteristics

Draw temperature	Draw efficiency	Ductility
$T_d < T_i$	high	low
$T_i < T_d < T_s$	high	high
$T_s < T_d$	low	high

CONCLUSIONS

The draw efficiency and rheology for uniplanar deformation of iPP have been examined by the elastic recovery test on melting and the compression yield energy experiment, respectively. There is a relation between draw efficiency and the existence of the smectic phase over a wide range of draw ($CR \sim 50$). To achieve high efficiency, it is necessary to select the draw temperature (T_d) below the smectic stability limit temperature (T_s). To obtain a highly drawn iPP, it is also necessary to select T_d above the intercept temperature at zero yield energy for the glassy phase (T_i). The window of T_d ($T_i < T_d < T_s$) for obtaining highly drawn iPP with high efficiency shifts to higher temperature by elevating the compression speed.

ACKNOWLEDGEMENT

The authors thank the National Science Foundation for support through CUMIRP at the University of Massachusetts.

REFERENCES

1 Saraf, R. F. and Porter, R. S. *J. Rheol.* 1987, **31**, 59
2 Guan, J. Y., Saraf, R. F. and Porter, R. S. *J. Appl. Polym. Sci.* 1987, **33**, 1517
3 Saraf, R. F. and Porter, R. S. *Polym. Eng. Sci.* 1988, **28**, 842
4 Watts, M. P. C., Zachariades, A. E. and Porter, R. S. *J. Mater. Sci.* 1980, **15**, 426
5 Porter, R. S., Daniels, M., Watts, M. P. C., Pereira, J. R. C., Deteresa, S. J. and Zachariades, A. E. *J. Mater. Sci.* 1981, **16**, 1134
6 Macosko, C. W. and Brand, G. J. *Polym. Eng. Sci.* 1972, **12**, 444
7 Starita, J. M. and Keaton, M. J. *SPE Tech. Papers* 1971, **29**, 67
8 Goldstein, M. *J. Chem. Phys.* 1969, **51**, 3728
9 Beatty, C. L. and Weaver, J. L. *Polym. Eng. Sci.* 1978, **18**, 1109
10 Hartmann, B. and Cole, R. F. *Polym. Eng. Sci.* 1983, **23**, 13
11 Roy, S. K., Kyu, T. and Manley, R. S. J. *Macromolecules* 1988, **21**, 499
12 Brandrup, J. and Immergut, E. H. 'Polymer Handbook', 2nd Edn, Wiley, New York, 1975
13 Bhateja, S. K. and Pae, K. D. *J. Macromol. Sci.* 1975, **C13**, 77
14 Oreilly, J. M. *J. Polym. Sci.* 1962, **57**, 429

APPENDIX

Relation between R(*1*) *and* R(*3*)

Volume conservation of sample (see *Figure 1*) gives

$$S_o d_o = S_c d_c = S_s d_s$$

$$S_c = S_o(d_o/d_c) = S_o CR \quad \text{(A1)}$$

$$\text{and } S_s = S_o(d_o/d_s) \quad \text{(A2)}$$

$$\text{where } CR = d_o/d_c$$

Substituting equations (A1) and (A2) into equation (1) yields

$$R(1) = \frac{S_o(d_o/d_c) - S_o(d_o/d_s)}{S_o(d_o/d_c) - S_o} \times 100$$

$$= \frac{CR - d_o/d_s}{CR - 1} \times 100$$

$$= \frac{d_c(CR - d_o/d_s)}{d_s - d_c} \frac{d_s - d_c}{d_c(CR-1)} \times 100 \quad \text{(A3)}$$

Substituting equation (3) into equation (A3) yields

$$R(1) = \frac{d_c\{CR - CR(d_c/d_s)\}}{d_s - d_c} R(3) \quad \text{(A4)}$$

where the real compression ratio (Cr) is defined as

$$Cr = d_s/d_c \quad \text{(A5)}$$

Substituting equation (A5) into equation (A4) yields

$$R(1) = CR \frac{(1 - Cr^{-1})}{Cr - 1} R(3) \quad (5)$$

Relation between R(*2*) *and* R(*3*)

Volume conservation of sample gives

$$\pi L_c^2 d_c = \pi L_o^2 d_o = \pi L_s^2 d_s$$

$$L_c = L_o(d_o/d_c)^{1/2} = L_o CR^{1/2} \quad \text{(B1)}$$

$$\text{and } L_s = L_o(d_o/d_s)^{1/2} \quad \text{(B2)}$$

Substituting equations (B1) and (B2) into equation (2) yields

$$R(2) = \frac{L_o(d_o/d_c)^{1/2} - L_o(d_o/d_s)^{1/2}}{L_o(d_o/d_c)^{1/2} - L_o} \times 100$$

$$= \frac{CR^{1/2} - (d_o/d_s)^{1/2}}{CR^{1/2} - 1} \times 100$$

$$= \frac{d_c\{CR^{1/2} - (d_o/d_s)^{1/2}\}(CR^{1/2}+1)}{d_s - d_c} \frac{d_s - d_c}{d_c(CR-1)} \times 100 \quad \text{(B3)}$$

Substituting equations (3) and (A5) into equation (B3) yields

$$R(2) = \frac{d_c\{CR^{1/2} - (d_o/d_s)^{1/2}\}(CR^{1/2}+1)}{Crd_c - d_c} R(3)$$

$$= \frac{\{CR^{1/2} - (CR/Cr)^{1/2}\}(CR^{1/2}+1)}{Cr - 1} R(3)$$

$$= (CR + CR^{1/2}) \frac{1 - Cr^{-1/2}}{Cr - 1} R(3) \quad (6)$$